ISBN: 978-3-95450-211-0 doi:10.18429/JACoW-SRF2019-MOP065

UPGRADE OF THE S-DALINAC INJECTOR CAPTURE SECTION*

S. Weih†, M. Arnold, J. Enders, N. Pietralla
Institut für Kernphysik, TU Darmstadt, Darmstadt, Germany
D. Bazyl, W.F.O. Müller, H. De Gersem
Institut für Theorie Elektromagnetischer Felder, TU Darmstadt, Darmstadt, Germany

Abstract

The superconducting injector section of the S-DALINAC (superconducting Darmstadt linear electron accelerator) [1] constists of two cryomodules with three 3-GHz SRF cavities in total. The first cavity of this pre-accelerator is currently a 5-cell structure designed for relativistic particle velocities. Since the gun delivers a 250 keV beam (β=0.74), this cavity is not suited for an efficient capture of the low-energy electron bunches provided by the normal-conducting section of the injector. Beam dynamics simulations and operational experience have shown a large low-energy tail in the phase-space distribution of the bunch downstream of the injector, which arises from the large phase-slippage during the capture in the 5-cell. It is therefore intended to replace the cavity with a β-adapted 6-cell, re-using most of the cryostat parts. This contribution presents the status of the injector upgrade and the layout and manufacturing status of the new cavity.

INTRODUCTION

The S-DALINAC (Fig. 1) [1] is a thrice-recirculating electron linear accelerator with a design energy of 130 MeV and a design beam current of 20 µA. It is operated in cw mode using elliptical 3-GHz 20-cell Niobium RF cavities at 2 K for acceleration. Recently, an ERL mode was implemented at the S-DALINAC using a path-length adjustment system in two of the recirculations [2, 3]. The beam is produced in a 250 keV thermionic gun. Additionally, a spin-polarized photo-gun is installed [4], this gun is currently being prepared for an upgrade to an acceleration voltage of 200 kV [5]. Downstream of the gun section, the beam is first shaped according to the 3 GHz time structure using a normal-conducting chopper and pre-buncher. The bunches are then accelerated up to 10 MeV in the superconducting part of the injector before entering the main LINAC. In its current state, the superconducting injector consists of two cryomodules containing a 5-cell and two 20-cell cavities, all with a geometrical β of 1. Operational experience as well as longitudinal beam dynamics simulations show that the energy spread of the beam is increased by phase slippage in the 5-cell due to the β-mismatch of the entering beam (β = 0.74) and the geometry of the cavity. In order to improve this capture of the electron bunches from both guns, a dedicated 6-cell capture cavity featuring a β of 0.86 was designed [6, 7]. It was decided to keep the overall length of the cavity fixed in order to re-use the existing cryostat. Surrounding components were adapted to the new geometry (Fig. 2) [8]. After finishing the design of the new cavity and ensuring the compatibility with the adapted cryomodule components, it was ordered from the manufacturer.

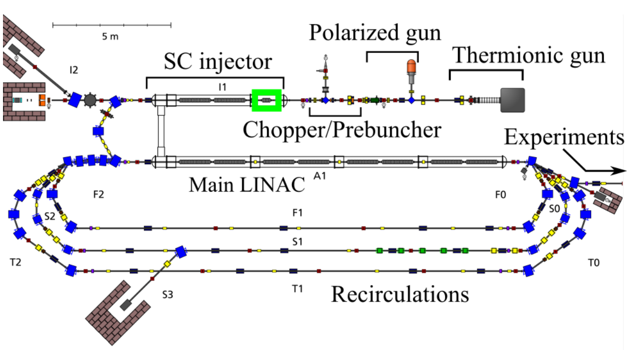

Figure 1: The S-DALINAC with indicated locations of the injector sections. The position of the superconducting capture structure is marked in green.

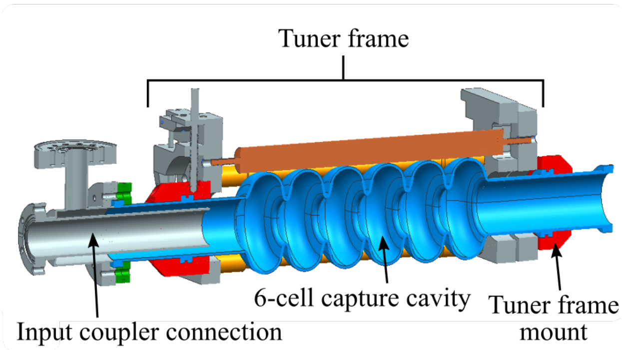

Figure 2: CAD model of the new 6-cell capture cavity with its surrounding components. More details on the adapted tuner frame can be found in [8].

CAVITY MANUFACTURING

Cavity Dimensions

Prior to the mechanical manufacturing of the cavity parts, the cavity dimensions had to be corrected to compensate the expected cool-down shrinkage as well as the material thickness planned to be removed from the inner surface during later BCP treatments (150 µm). Since only one cavity will be fabricated, there is no prototype cavity available for test measurements. The frequency shifts induced by the two processes thus had to be estimated. The considered values for the frequency shift estimations are summarized in Tables 1 and 2. For the cool-down shrinkage, the values available from the latest cavity production for the S-DALINAC are consistent with the measured fre-

* work supported by DFG through GRK 2128 "AccelencE"
† sweih@ikp.tu-darmstadt.de

ISBN: 978-3-95450-211-0 doi:10.18429/JACoW-SRF2019-MOP065

quency shift for 3.9 GHz XFEL cavities [9] scaled to 3 GHz. A theoretical calculation using the integrated thermal contraction coefficient of niobium confirms the frequency shift. Therefore a reliable estimate of 4.5 MHz

Table 1: Considered Values for the Cool-down Frequency Shift Estimation From 300 K to 2 K

Method / Cavity Type	Δf (MHz)
Calculated from thermal contraction	4.3
3.9 GHz XFEL cavities [9], scaled to 3 GHz	4.7
S-DALINAC 20-cells (RI series) [10]	4.5
Average	4.5 ± 0.3

Table 2: Considered Values for the Estimation of the Frequency Shift Induced by a 150 µm BCP Treatment

Cavity Type	Δf (MHz)
S-DALINAC 20-cells (Dornier series)	-3.8 MHz
S-DALINAC 20-cells (RI series)	-3.4 MHz
Average	-3.6 ± 0.2

can be obtained. 150 µm BCP correspond to an average frequency shift of -3.6 MHz using data from different series of S-DALINAC 20-cells. However, the considered cavity types feature slightly different cell geometries compared to the new 6-cell, whose cell shape [7] is adapted from the TESLA-type. Recently produced 3 GHz single-cell test cavities [11] show a much higher BCP sensitivity of -5.6 MHz for 150 µm, but again the cell shape is different since thiese cavities are made from two endgroups. Because no 6-cell cavity with similar layout to the new structure is available for comparison, the estimated value is not reliable. However, it was concluded that the cool-down and BCP frequency shift approximately compensate each other. Therefore it was decided to use the inner dimensions of the design model (2 K, with final dimensions after BCP) as starting point for the mechanical manufacturing. The target resonance frequency in the warm state of the cavity before BCP then corresponds to the operational target frequency of 2.9972 GHz, accordingly. In order to ensure the correct target frequency after the surface treatment, the BCP will be conducted in two steps with an intermediate field-flatness tuning and cool-down test in the vertical test cryostat at S-DALINAC [11]. The final amount of material to be removed can than be determined from the measured cool-down frequency shift together with the obtained BCP sensitivity.

Dumbbell Trimming

After the mechanical manufacturing of the single cavity components, dumbbells and endgroups are produced by electron-beam welding. These parts are manufactured with an overlength and then successively trimmed towards the desired target frequency in order to ensure the correct resonance frequency of the assembled cavity in the end. For the preparation of this process, the trimming sensitivities and the influence of the welding preparation were simulated using CST microwave studio [12]. Figure 3 shows the simulated trimming sensitivity for a regular dumbbell which was determined to 18.3 MHz/mm. From the simulations, target frequencies for the trimming process were derived. A similar simulation was conducted for the endgroups. The dumbbell trimming is expected to be performed in summer 2019.

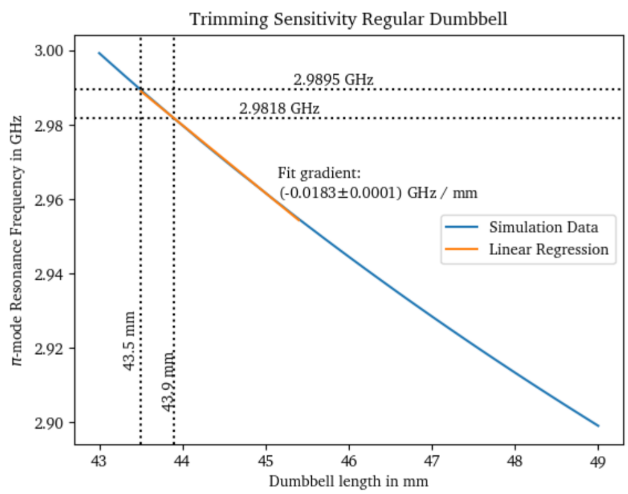

Figure 3: Simulated trimming frequency sensitivity for a regular dumbbell of the new 6-cell structure. A gradient of 18.3 MHz/mm was obtained. The dashed lines indicate the target length of the dumbbell with (43.9 mm) and without (43.5 mm) additional material for weld shrinkage compensation and the corresponding target frequencies.

DIAGNOSTICS UPGRADE

Beam dynamics simulations of the injector beam have shown that the energy spread induced in the capture structure strongly depends on the input bunch length. It is therefore foreseen to add a diagnostics section in front of the superconducting injector for a better characterization of the beam downstream the chopper and prebuncher section. An existing vertical bamline can be re-used for this purpose. Figure 4 shows the concept of this setup. In the first stage, it consists of a vertical bending dipole and a diagnostics chamber for profile and current measurements located in the dispersive region after some drift space. A quadrupole (or triplet) could be added later to manipulate the dispersion variably. From the energy-spread measurement the velocity difference between the head and tail of the bunch can be derived, which enables an estimate for the bunched beam length at the capture structure entry. In addition, it is planned to install a normal-conducting transverse deflecting cavity to the diagnostics section later to obtain a dedicated bunch-length measurement setup.

ISBN: 978-3-95450-211-0 doi:10.18429/JACoW-SRF2019-MOP065

CONCLUSION AND OUTLOOK

A superconducting 6-cell reduced-β capture cavity is currently being manufactured for the S-DALINAC capture section. The new structure will improve the injector beam quality and is suited for both the 250 keV thermionic gun and the spin-polarized photo-gun after its upgrade to 200 keV. For the cavity manufacturing, cool-down and BCP frequency shifts were estimated. Dumbbell and endgroup trimming sensitivity simulations were conducted and target frequencies obtained. Additionally, a new diagnostics setup is planned to improve the characterization of the beam downstream the chopper/pre-buncher section. This setup is expected to be used for an optimization of the bunch length at the capture section entry during operation, which will be highly beneficial for the commissioning of the upgraded injector. The cavity delivery is expected end of 2019. After a final surface preparation, the cavity would then be ready for installation during the maintenance shut-down early 2020. In parallel to the cavity manufacturing, the diagnostics setup will be installed.

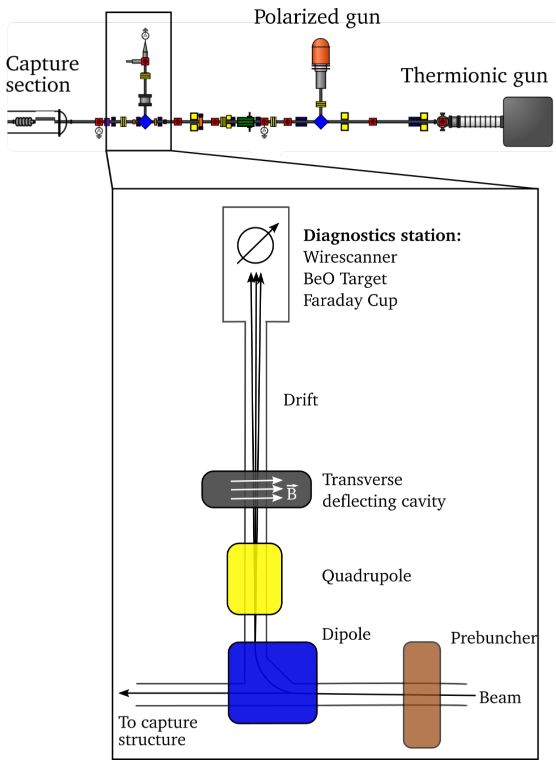

Figure 4: Concept of the new diagnostics setup planned to be used for the characterization of the beam in front of the superconducting capture section.

REFERENCES

[1] N. Pietralla, "The Institute of Nuclear Physics at the TU Darmstadt", in *Nuclear Physics News*, vol. 28, no. 2, pp. 4-11, 2018.

[2] M. Arnold *et al.*, "ERL Mode of S-DALINAC: Design and Status", in *Proc. 59th Advanced ICFA Beam Dynamics Workshop on Energy Recovery Linacs (ERL'17)*, Geneva, Switzerland, Jun. 2017, pp. 40-44. doi:10.18429/JACoW-ERL2017-MOIDCC006

[3] M. Arnold *et al.*, "First ERL Operation of S-DALINAC and Commissioning of a Path Length Adjustment System", in *Proc. 9th Int. Particle Accelerator Conf. (IPAC'18)*, Vancouver, Canada, Apr.-May 2018, pp. 4859-4862. doi:10.18429/JACoW-IPAC2018-THPML087

[4] Y. Poltoratska *et al.*, "Status and recent developments at the polarized-electron injector of the superconducting Darmstadt electron linear accelerator S-DALINAC", in *J. Phys: Conf. Ser.,* vol 298, no. 1, pp. 012002, 2011.

[5] M. Herbert, J. Enders, Y. Fritzsche, N. Kurichiyanil, and V. Wende, "Inverted Geometry Photo-Electron Gun Research and Development at TU Darmstadt", in *Proc. 9th Int. Particle Accelerator Conf. (IPAC'18)*, Vancouver, Canada, Apr.-May 2018, pp. 4545-4547. doi:10.18429/JACoW-IPAC2018-THPMK101

[6] D. Bazyl, H. De Gersem, and W. F. O. Müller, "Upgrade of the Capture Section of the S-DALINAC Injector", in *Proc. 8th Int. Particle Accelerator Conf. (IPAC'17)*, Copenhagen, Denmark, May 2017, pp. 993-995. doi:10.18429/JACoW-IPAC2017-MOPVA055

[7] D. Bazyl, H. De Gersem, W. F. O. Müller, J. Enders, and S. Weih, "A 3 GHz SRF Reduced-beta Cavity for the S-DALINAC", in *Proc. 9th Int. Particle Accelerator Conf. (IPAC'18)*, Vancouver, Canada, Apr.-May 2018, pp. 3838-3840. doi:10.18429/JACoW-IPAC2018-THPAL081

[8] S. Weih *et al.*, "Development of an Improved Capture Section for the S-DALINAC Injector", in *Proc. 29th Linear Accelerator Conf. (LINAC'18)*, Beijing, China, Sep. 2018, pp. 68-70. doi:10.18429/JACoW-LINAC2018-MOPO018

[9] P. Pierini *et al.*, "Fabrication of the 3.9 GHz SRF Structures for the European XFEL", in *Proc. 17th Int. Conf. RF Superconductivity (SRF'15)*, Whistler, Canada, Sep. 2015, paper THPB035, pp. 1162-1165.

[10] T. Kuerzeder *et al.*, "Development and Test of a New Cryostat Module for the Injector of the S-DALINAC", in *Proc. 16th Int. Conf. RF Superconductivity (SRF'13)*, Paris, France, Sep. 2013, paper MOP082, pp. 334-336.

[11] R. Grewe *et al.*, "Superconducting RF Cavity Materials Research at the S-DALINAC", presented at the 19th Int. Conf. RF Superconductivity (SRF'19), Dresden, Germany, Jun.-Jul. 2019, paper MOP022.

[12] CST Studio, https://www.cst.com